Hindawi Publishing Corporation
Journal of Chemistry
Volume 2015, Article ID 826358, 9 pages
http://dx.doi.org/10.1155/2015/826358

Research Article

Effect of High Temperature on the Electrochemical and Optical Properties of Emeraldine Salt Doped with DBSA and Sulfuric Acid

Salma Gul,[1] Anwar-ul-Haq Ali Shah,[2] and Salma Bilal[1]

[1]*National Centre of Excellence in Physical Chemistry, University of Peshawar, Peshawar 25120, Pakistan*
[2]*Institute of Chemical Sciences, University of Peshawar, Peshawar 25120, Pakistan*

Correspondence should be addressed to Salma Bilal; dresalmabilal@gmail.com

Received 7 December 2014; Accepted 18 January 2015

Academic Editor: Tomokazu Yoshimura

A comprehensive study of thermally treated polyaniline in its emeraldine salt form is presented here. It offers an understanding of the thermal stability of the polymer. Emeraldine salt was prepared by a novel emulsion polymerization pathway using dodecylbenzene sulfonic acid and sulfuric acid together as dopants. The effect of temperature and heating rate on the degradation of this emeraldine salt was studied via thermogravimetric analysis. The thermally analyzed sample was collected at various temperatures, that is, 250, 490, 500, and 1000°C. The gradual changes in the structure of the emeraldine salt were followed through cyclic voltammetry, Fourier transform infrared spectroscopy, and ultraviolet-visible spectroscopy. Results demonstrate that emeraldine salt shows high thermal stability up to 500°C. This is much higher working temperature for the use of emeraldine salt in higher temperature applications. Further heat treatment seems to induce deprotonation in emeraldine salt. Cyclic voltammetry and ultraviolet-visible spectroscopy revealed that complete deprotonation takes place at 1000°C where it loses its electrical conductivity. It is interesting to note that after the elimination of the dopants, the basic backbone of emeraldine salt was not destroyed. The results reveal that the dopants employed have a stability effect on the skeleton of emeraldine salt.

1. Introduction

With the passage of time, polyaniline is going on to be established as one of the most important conductive polymers due to its high conductivity in doped state, high redox reversibility, easy transformation in colored films, and high stability in the environment [1]. Among the four different oxidation forms of polyaniline, leucoemeraldine (fully reduced), pernigraniline (fully oxidized), and emeraldine base (half oxidized and half reduced) are insulating while emeraldine salt is the only conducting form [2]. Special electronic, optical, magnetic, and mechanical properties allow the use of emeraldine salt in a large number of potential applications such as corrosion protections of metals [3, 4], rechargeable batteries [5], capacitors [6], and sensors [7]. However, the stiffness of its backbone and strong intermolecular interactions between adjacent chains limit its processability in organic solvents [8, 9]. This protonated emeraldine salt is also reported to be less thermally stable than the emeraldine base form and its thermal stability varies with the type of dopant [10].

The awesome potentials of emeraldine salt in technologies have forced the scientific community to improve the solubility/processability (much needed property for its commercial applications) of these materials by adopting different pathways for synthesis. The successful strategies include the synthesis of substituted polyaniline [11, 12], copolymerization of aniline with substituted anilines [13], and synthesis of emeraldine salt by emulsion/inverse emulsion polymerization technique [14, 15]. However, there are only few systematic studies on the thermal degradation behavior of emeraldine salt. Detailed knowledge of thermal stability and degradation behavior is particularly important for its effective use in electronic devices, solid state batteries, chemical sensors, electromagnetic shielding, anticorrosion coatings, and so forth [16].

For improving thermal stability, various methods were developed. Paul and Pillai [17] investigated thermal properties of emeraldine salt doped with functionalized sulfonic acid. These protonated polymers were stable up to 200°C. Chen [18] compared the thermal stability of emeraldine base and emeraldine salt. The highest thermal degradation temperature of emeraldine salt was found to be 410°C while for emeraldine base it was 450°C. Ansari and Keivani [19] synthesized emeraldine salt in the presence of different bronsted acids such as hydrochloric acid (HCl), sulfuric acid (H_2SO_4), and 8-hydroxypyrene-1,3,6-trisulfonate (HPTS). They found that thermal stability of the synthesized emeraldine salt was highly dependent on the nature and size of the dopant used. According to their TGA results, emeraldine salts doped with HCl, H_2SO_4, and HPTS were thermally stable up to 200°C, 320°C, and 250°C, respectively. Brožová et al. [20] performed stability test for emeraldine base by using TGA. They reported thermal stability of the synthesized emeraldine base up to 350°C. Bompilwar et al. [21] performed a series of experiments for improving thermal stability of emeraldine salt. They prepared nanocomposites of emeraldine salt by varying the weight percent of CdS/ZnS during polymerization of aniline. They achieved thermal stability up to 300°C. Ansari and Mohammad [22] reported the synthesis of nanocomposite of emeraldine salt with TiO_2 using NMP as a solvent. These composites were found to be thermally stable up to ~400°C. Recently, Qiang et al. [23] synthesized a hyperbranched emeraldine salt through a ring-opening reaction between hyperbranched polysiloxane and emeraldine salt. The structure and properties of hyperbranched emeraldine salt were also characterized. The properties of hyperbranched emeraldine salt had significantly improved compared with only emeraldine salt. Specifically, emeraldine salt was only soluble in polar solvents, while hyperbranched emeraldine salt also showed improved solubility in weak polar or nonpolar solvents such as tetrahydrofuran and CH_2Cl_2. Similarly the initial decomposition temperature of hyperbranched emeraldine salt was 360°C, about 78°C higher than that of PA (282°C).

All the above studies reveal that the method of synthesis is important in determining the thermal stability of the polymer. Generally a three-step decomposition process has been observed for the emeraldine salt [9, 19]. In this process the initial stage of weight loss is due to the volatilization of water molecules; then at higher temperatures the protonic acid component of the polymer is lost and finally at more extreme temperatures the degradation of the polymer can lead to production of gases such as acetylene and ammonia or amorphous carbon [19, 24].

In order to cope with the problems related to the poor processability and low thermal stability of the emeraldine salt form of PANI, we started a systematic study aimed at establishing effective polymerization routs for the synthesis of processable emeraldine salts. Previously, we developed a novel inverse emulsion polymerization pathway for the synthesis of completely soluble and highly thermally stable (~500°C) emeraldine salts [15]. In the present work thermal stability of emeraldine salt is evaluated in more detail. The emeraldine salt was synthesized by another very fruitful emulsion polymerization method [25] using dodecylbenzenesulfonic acid (DBSA) as surfactant and dopant. In this pathway, sulfuric acid (H_2SO_4) was used as codopant for the first time. The synthesized salts showed very good solubility in a large number of organic solvents, exhibited very good electrochemical activity and electrochromics reversibility, and were highly conducting. These salts also showed excellent protection efficiency for steel. In the present work a further attempt is made to determine the effects of dopants on the thermal stability of emeraldine salt form of polyaniline in more detail and to assess its processing temperature. For this purpose thermogravimetric analysis (TGA), cyclic voltammetry (CV), UV-Vis spectroscopy, and Fourier transform infrared spectroscopy (FT-IR) were used to study these properties. The thermal, electrochemical, and optical studies suggested 500°C as the processing temperature of the emeraldine salt. Moreover, the basic backbone of the emeraldine salt remained stable at very high temperature, that is, 1000°C. This is quite high thermal stability of the emeraldine salt compared to the previous reports as discussed above.

2. Experimental

2.1. Materials and Chemicals. All chemicals were of analytical grade. Aniline (Riedel-de Häen) was distilled under reduced pressure and stored in a refrigerator. H_2SO_4 (Riedel-de Häen), chloroform (Scharlau), dodecylbenzenesulfonic acid (DBSA) (Aldrich), and ammonium persulfate (Riedel-de Häen) were used as received. Water (Millipore) was used for solution preparation.

2.2. Synthesis of Emeraldine Salt. Emeraldine salt was prepared by the method reported elsewhere [25]. In a typical experiment, DBSA was slowly added to 50 mL of chloroform with constant stirring. Aniline was afterwards added to the above mixture. It was followed by the dropwise addition of the codopant H_2SO_4 and of an aqueous solution of ammonium persulfate, in order to get a milky white emulsion. The content of the round-bottom flask gradually turned green and the stirring was continued at room temperature. After about 24 hours the reaction was stopped; the organic phase was separated and washed repeatedly with deionized water. It was then added to 200 mL of acetone to precipitate out the polymer. The green precipitate obtained was filtered, washed with excess of acetone, and dried overnight in an oven at 60°C.

The reaction parameters were optimized by varying the amounts of reactants. Maximum yield of emeraldine salt was obtained at 7.47 mmol DBSA, 12.5 mmol H_2SO_4, 1.25 mmol ammonium persulfate, and 10.95 mmol aniline. The products obtained at these amounts were used for the present study.

2.3. Heat Treatment. Emeraldine salt in the form of emeraldine salt was subjected to heat treatment using thermogravimetric analysis (TGA). Thermal analysis of the polymer was carried out by using Perkin Elmer (USA) at a heating rate of 10°/min in the presence of N_2 atmosphere. The material was

subjected to a controlled temperature (from 30 to 1000°C) and its mass was monitored as a function of temperature. The sample was collected at the offset of each weight loss stage (i.e., 250, 500, and 1000°C). Thermally analyzed sample was also collected at 490°C (before the end of second weight loss stage) because we were more interested in the dopants effect on the thermal stability of the polymer.

2.4. Characterizations. Cyclic voltammetry was performed with a Reference 3000 ZRA potentiostat/galvanostat. All experiments were performed at room temperature in a three-electrode cell. Emeraldine salt dissolved in tetrahydrofuran was dip-coated onto a gold disc which was used as working electrode. A gold coiled wire and a saturated calomel electrode (SCE) were used as counter and reference electrodes, respectively. Cyclic voltammograms were recorded in 0.5 M H_2SO_4.

Fourier transform infrared (FT-IR) spectra of emeraldine salt samples were obtained using Shimadzu (Japan) spectrometer in the range of 400–4000 cm^{-1} by using KBr pellets.

UV-Vis spectra were recorded with a Perkin Elmer 650 (UK) spectrophotometer. Samples of emeraldine salt were dissolved in tetrahydrofuran.

3. Results and Discussion

3.1. Thermogravimetric Analysis (TGA). TGA is considered as one of the most useful techniques for evaluating the onset of thermal decomposition temperature and determining thermal stability of conducting polymers. In the present study, thermogram (Figure 1) of the emeraldine salt shows a three-step decomposition scenario similar to the previous reports [9, 19].

In order to assess the stepwise change in the polymer make-up, the thermally analyzed sample was collected at each focal step and its properties were investigated by various techniques as follows.

3.2. Electroactivity. The electroactivity/redox properties of the emeraldine salt thermally treated at different temperatures was investigated by cyclic voltammetry and is presented in Figure 2. Cyclic voltammogram of the as-synthesized emeraldine salt shows typical redox electrochemistry of emeraldine salt [26].

The peaks at E_{SCE} = 0.32 V and E_{SCE} = 0.75 V correspond to the transformation of leucoemeraldine to emeraldine salt and emeraldine salt to pernigraniline, respectively. On the reverse scan, peaks E_{SCE} = 0.61 V and E_{SCE} = 0.05 V correspond to the conversion of pernigraniline to emeraldine salt and emeraldine salt to leucoemeraldine, respectively, given our reference [15, 27]. Interestingly it can be noted that after thermal treatment (at 250, 490, and 500°C), the intensity of the redox peaks increases which show very good electroactivity of the emeraldine salt, synthesized in the present work, at elevated temperatures. This might be due to the thermal doping of some undoped dopant molecules in the emeraldine salt matrix [28]. At high temperatures, the thermal movements of the material make the previously inaccessible regions of emeraldine salt available for additional doping [28]. When emeraldine salt is doped additionally by heating, it may experience a change in structure. This resulted in the formation of layered structure of the emeraldine salt arranged with dopants moieties and thus increases its electroactivity [28]. However, a middle redox peak appears in-between the two redox processes for emeraldine salt heated at 490 and 500°C. This peak is assigned to some degradation products of emeraldine salt [29]. On further heating at 1000°C, these characteristic peaks almost disappear. As discussed in the following FT-IR section the emeraldine salt lost its dopant at this temperature and thus lost its electroactivity.

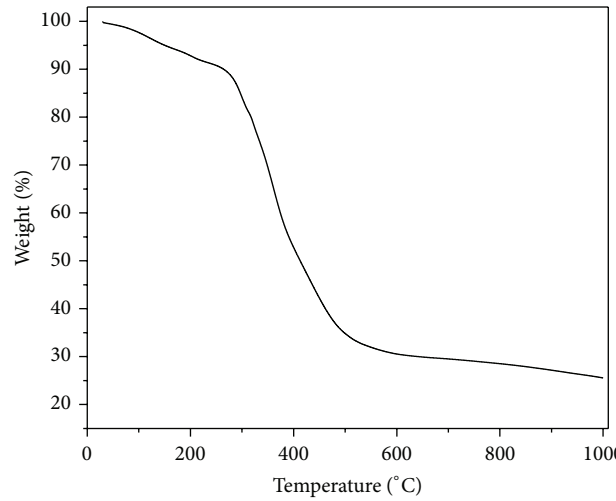

Figure 1: Thermogravimetric curve for emeraldine salt.

3.3. FT-IR Spectroscopy. The structural changes of the emeraldine salt during heating process were followed by FT-IR spectroscopy. The spectra are shown in Figure 3 and their band assignments are listed in Table 1. The infrared spectrum of the as-synthesized emeraldine salt is similar to that obtained by other authors [24, 30–34]. The characteristic infrared bands at about 1615 cm^{-1} and 1494 cm^{-1} are assigned to the quinoid and benzenoid stretching vibrations, respectively. A broad band at 3440 cm^{-1} corresponds to the N–H stretching vibration. The band at about 3021 cm^{-1} is assigned to a C–H stretching vibration of the benzene rings. The 1295 cm^{-1} band is due to the C–N stretching of an aromatic amine while the band at 1300 cm^{-1} is attributed to the stretching vibration of C–N in the quinoid imine unit [35]. The –OH stretching vibration of water appeared at 3500–3700 cm^{-1} part of the spectrum. The double bands near 2947 and 2878 cm^{-1} are attributed to stretching vibrations of the aliphatic C–H. This indicates the existence of the alkyl chain in the emeraldine salt backbone. This peak confirms the presence of DBSA in the emeraldine salt system [33]. The band for HSO_4 appeared at 613 cm^{-1} which is responsible for the acid dopant in the chain of emeraldine salt.

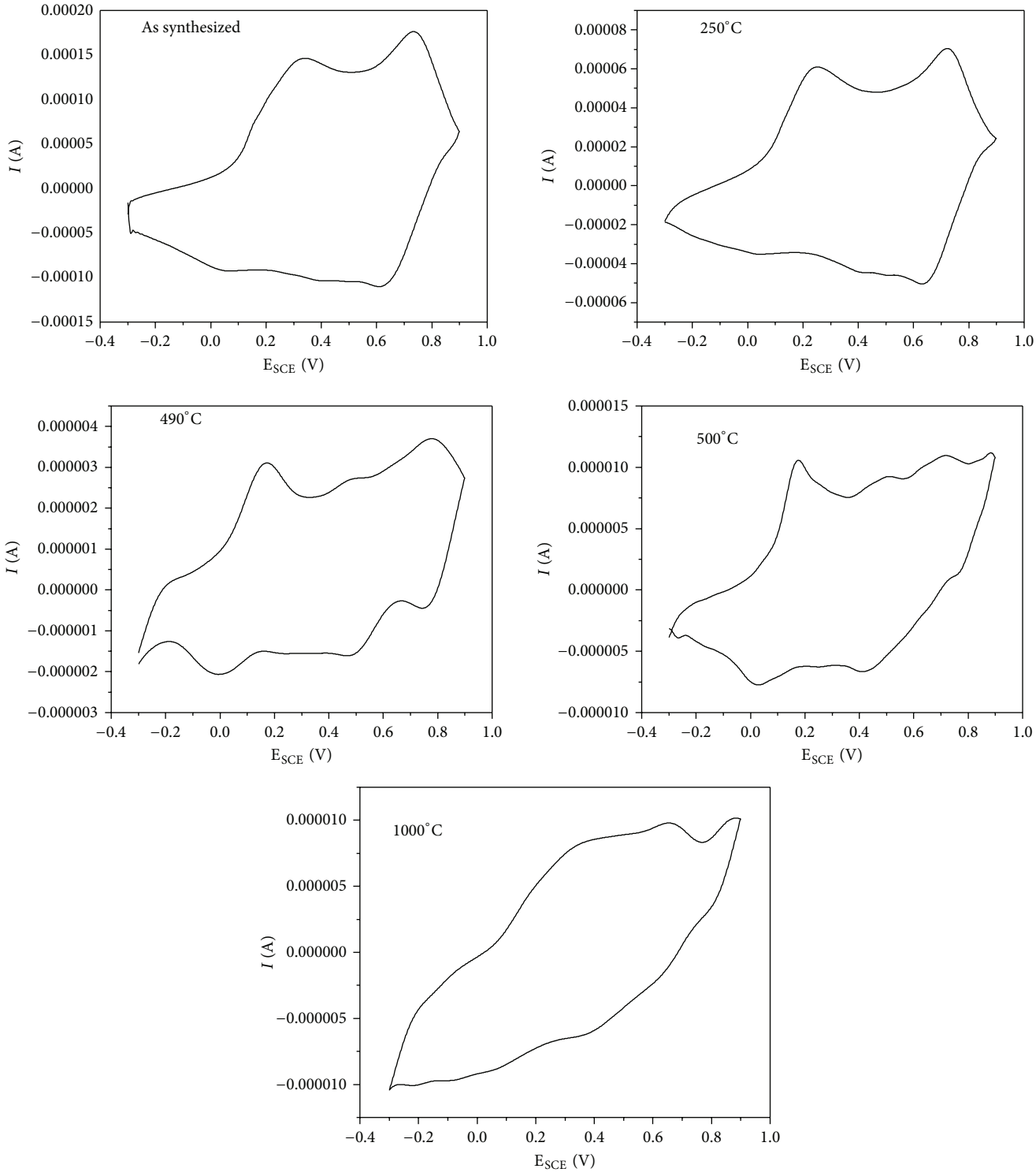

Figure 2: CVs of emeraldine salt on a gold disc electrode (versus SCE) in 0.5 M H_2SO_4. The sample is treated at various temperatures as indicated.

These results suggest that this polymerization pathway leads to incorporation of both surfactant and acid group onto the emeraldine salt as dopants (Figure 4(a)).

After thermal treatment at 250°C and 490°C the infrared spectra of the sample remain unchanged. The major peaks and their positions were found to remain essentially the same. These results confirmed that the structure of emeraldine salt persists at these temperatures (Figures 4(b)-4(c)).

When this emeraldine salt was further heated up to 500°C, the peaks at 2947 and 2878 cm^{-1} become weak due

Table 1: Vibrational bands in FT-IR spectra of emeraldine salt.

As-synthesized emeraldine salt	Heat treated emeraldine salt at				Band assignment
	250°C	490°C	500°C	1000°C	
1615	1615	1615	1615	1615	Quinoid
1494	1494	1494	1494	1494	Benzenoid
3440	3440	3440	3440	3440	N–H stretching vibration
3021	3021	3021	3021	3021	C–H stretching vibration of benzene
1300	1300	1300	1300	1300	C–N stretching vibration of quinoid imine
1295	1295	1295	1295	1295	C–N stretching vibration of aromatic amine
2947 and 2878	2947 and 2878	2947 and 2878	2947 and 2878	—	Stretching vibrations of the aliphatic C–H (DBSA)
613	613	613	613	—	HSO_4 (from acid dopant)
3500–3700	3500–3700	3500–3700	3500–3700	—	OH stretching vibration of water

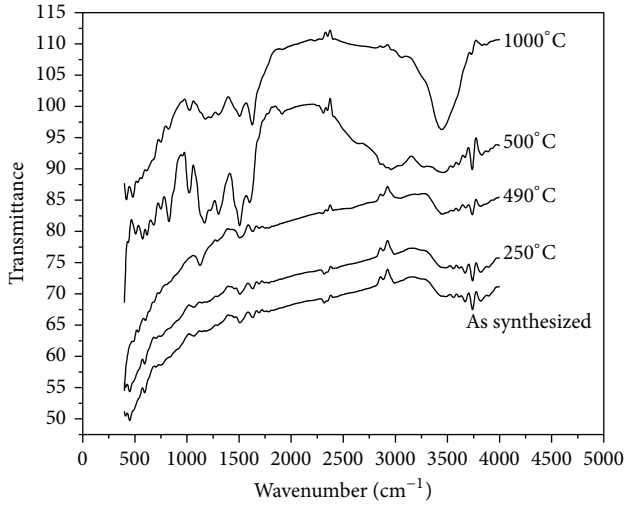

Figure 3: FT-IR spectra of untreated and heat treated emeraldine salt.

to the onset of degradation of some of the alkyl chain of DBSA. However, the intensity of the characteristic band for benzenoid stretching vibrations increased. As discussed in Section 3.2, at high temperature, thermal doping of some undoped molecules (dopants) takes place in the emeraldine salt matrix [28]; as a consequence, benzenoid band becomes more prominent. Beside this, other characteristic bands were also found to remain the same in the FT-IR spectrum which reveal that the basic structure, emeraldine salt, is still stable at high temperature, that is, 500°C (Figure 4(d)).

The spectrum of the sample, collected at 1000°C, is greatly changed. The bands in range of 3500–3700 cm^{-1} are eliminated from the spectrum due to the H-bonds breaking. This could be caused by the loss of residual water at higher temperature [24]. Intensity of C–N stretching band increased at this elevated temperature. This suggests the occurrence of deprotonation process [36]. Similarly, the double bands near 2947 and 2878 cm^{-1} symmetric stretching vibration disappear due to the degradation of DBSA at high temperature. Moreover, the band for HSO_4 (at 613 cm^{-1}) also almost vanished. At the same time the peak intensity of quinoid stretching bands increases as compared to benzenoid band, indicating the conversion of some benzenoid rings to quinoid rings. These changes are also connected to deprotonation process and a shorter effective conjugation length of the backbone of emeraldine salt [36]. However, the presence of characteristic bands for quinoid to benzoid rings, C–N, N–H, and C–H stretching vibrations, indicates that, even at this very high temperature of 1000°C, the basic backbone of the emeraldine salt remained stable and does not show any evidence of its complete degradation to gases/amorphous carbon as described by other reports [19, 24] (Figure 4(e)). These results further encourage us to assume that the strategy of using two different dopants at the same time is successful enough to provide good thermal stability to structure of the emeraldine salt.

3.4. UV-Vis Spectroscopy. The above-mentioned observations, assumptions, and discussion were further supported by recording the UV-Vis spectra for emeraldine salt (Figure 5 and Table 2). The UV-Vis spectrum of the as-synthesized emeraldine salt shows three characteristic absorption peaks at 345, 440, and 790 nm wavelength. The first band arises from π-π^* electron transition within benzoid (B) ring of

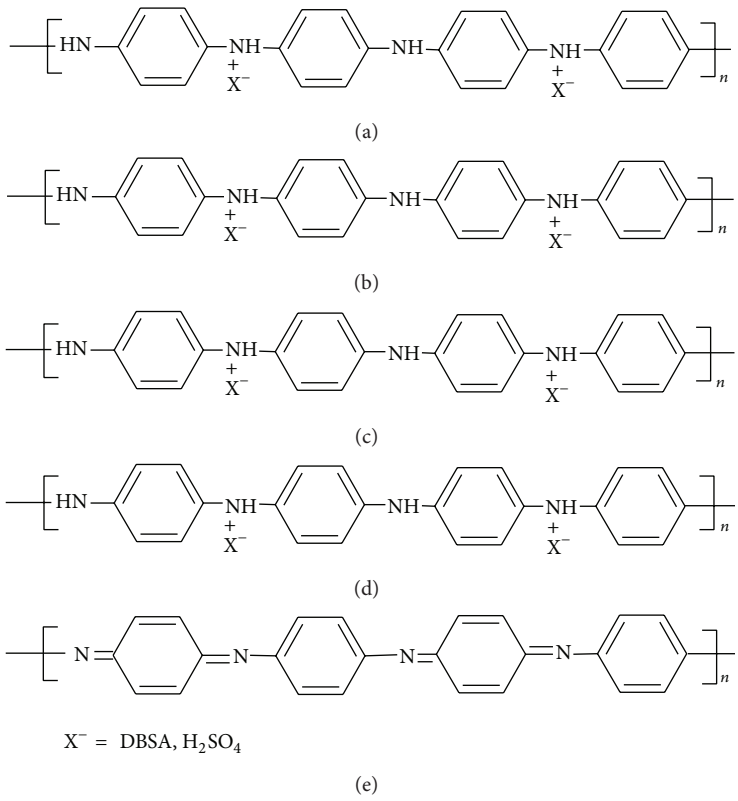

Figure 4: Proposed structures of (a) as-synthesized emeraldine salt and heat treated samples of emeraldine salt up to (b) 250°C, (c) 490°C, (d) 500°C, and (e) 1000°C.

the polymer backbone; the second and third absorption bands are assigned to the polaron-π^* transition (quinoid "Q" ring) and π-polaron transition (Exciton), respectively [9, 37]. The second and third peaks are related to the doping level and formation of polaron which support the formation of emeraldine salt [38]. As also observed in CV and FTIR studies, after thermal treatment at 250°C and 490°C the UV-Vis spectra of the sample remain unchanged. Thereafter, heating up to 500°C, some changes developed in the spectrum of emeraldine salt. On further heating substantial, changing features are observed in the UV-Vis spectrum of the sample thermally treated up to 1000°C. The position and the absorbance of the band at 345 nm are affected with thermal treatment. The increase in temperature increases the absorbance of this band exhibiting a blue shift because of deprotonation and transformation of emeraldine from conducting to insulating state. The band at 420 nm, assigned to the polaron transition, also became weak at 500°C and disappears at high temperature (1000°C). Furthermore, at elevated temperature, the decrease of the band at around 790 nm may be attributed to the decrease in protonation of the polymer backbone which results in the decrease of the number of polarons. These results are supported by FT-IR spectroscopy which indicated that heating influences the protonation of emeraldine salt. In the light of these studies we can safely assume that the emeraldine salt is stable up to 500°C which is quite high temperature for emeraldine salt.

4. Conclusions

The thermal stability of emeraldine salt form of polyaniline, synthesized via a novel emulsion polymerization route [25], was carried out in order to identify the optimum processing/working temperature suitable for various applications. Emeraldine salt undergoes various structural changes when exposed to an elevated temperature. These are manifested by the decreasing mass of the samples, degradation of dopants, and decreasing content of hydrogen bonding. The structural changes in emeraldine salt were assessed with FT-IR spectroscopy. The results indicate that up to 500°C the basic structure is retained as major peaks and their positions were found to remain essentially the same. At 1000°C, emeraldine salt loses all its dopants molecules. However the basic skeleton is retained even at 1000°C. The results suggest that although the dopants are eliminated early, their presence in the beginning has a stability effect on the backbone of emeraldine salt. Cyclic voltammetry and UV-Vis spectroscopy also support these results and suggest 500°C as optimum working temperature for the synthesized emeraldine salt. The results indicate that the codoping strategy adopted for the synthesis of this salt form of polyaniline is servable enough that both dopants were effectively incorporated in the chain of emeraldine salt which results in the highest thermal stability compared to the reported literature. This highest thermal stability

Table 2: Band positions (λ) in the UV-Vis spectra of emeraldine salt.

Temperature (°C)	π-π^* transition λ (nm)	Polaron-π^* λ (nm)	π-polaron transition λ (nm)
As synthesized	351	440	790
250	347	440	790
490	345	440	790
500	288	440	639
1000	286	—	—

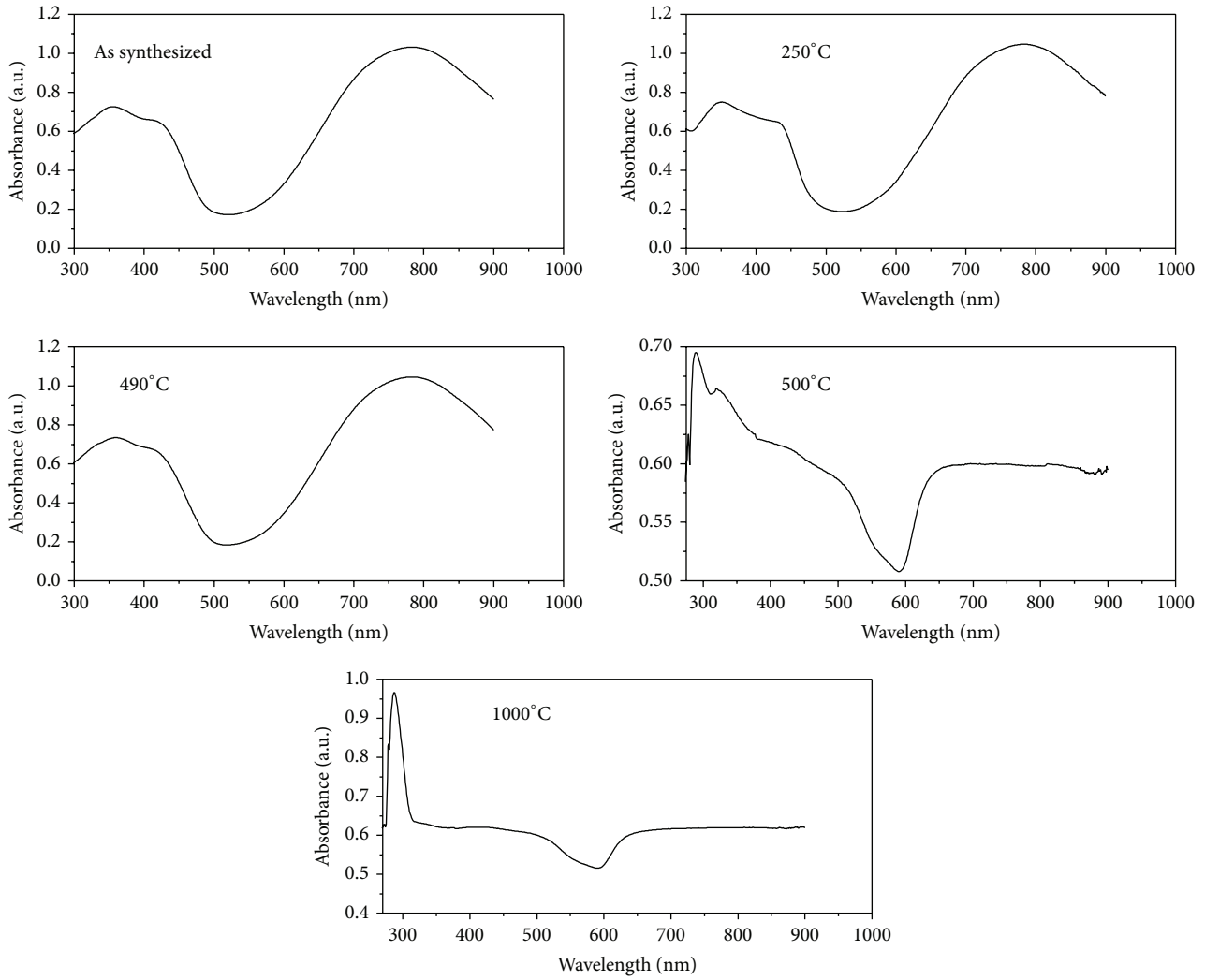

Figure 5: UV-Vis spectra of emeraldine salt samples recorded in tetrahydrofuran (THF) solvent. The sample is treated at various temperatures as indicated.

makes this polymer a good candidate for application in electronic devices, solid state batteries, chemical sensors, electromagnetic shielding, anticorrosion coatings, and so forth.

Conflict of Interests

The authors declare that there is no conflict of interests regarding the publication of this paper.

Acknowledgment

Financial support from Higher Education Commission, Islamabad, Pakistan, is gratefully acknowledged under Project no. 20-1647.

References

[1] P. S. Rao and D. N. Sathyanarayana, "Synthesis of electrically conducting copolymers of aniline with o/m-amino benzoic acid

by an inverse emulsion pathway," *Polymer*, vol. 43, no. 18, pp. 5051–5058, 2002.

[2] C. L. Gettinger, A. J. Heeger, D. J. Pine, and Y. Cao, "Solution characterization of surfactant solubilized polyaniline," *Synthetic Metals*, vol. 74, no. 1, pp. 81–88, 1995.

[3] A. B. Samui, A. S. Patankar, J. Rangarajan, and P. C. Deb, "Study of polyaniline containing paint for corrosion prevention," *Progress in Organic Coatings*, vol. 47, no. 1, pp. 1–7, 2003.

[4] A. H. El-Shazly and H. A. Al-Turaif, "Improving the corrosion resistance of buried steel by using polyaniline coating," *International Journal of Electrochemical Science*, vol. 7, no. 1, pp. 211–221, 2012.

[5] L. Xiao, Y. Cao, J. Xiao et al., "A soft approach to encapsulate sulfur: polyaniline nanotubes for lithium-sulfur batteries with long cycle life," *Advanced Materials*, vol. 24, no. 9, pp. 1176–1181, 2012.

[6] H. R. Ghenaatian, M. F. Mousavi, and M. S. Rahmanifar, "High performance battery-supercapacitor hybrid energy storage system based on self-doped polyaniline nanofibers," *Synthetic Metals*, vol. 161, no. 17-18, pp. 2017–2023, 2011.

[7] C. Liu, K. Hayashi, and K. Toko, "Au nanoparticles decorated polyaniline nanofiber sensor for detecting volatile sulfur compounds in expired breath," *Sensors and Actuators, B: Chemical*, vol. 161, no. 1, pp. 504–509, 2012.

[8] B. C. Roy, M. D. Gupta, L. Bhoumik, and J. K. Ray, "Spectroscopic investigation of water-soluble polyaniline copolymers," *Synthetic Metals*, vol. 130, no. 1, pp. 27–33, 2002.

[9] Y.-G. Han, T. Kusunose, and T. Sekino, "One-step reverse micelle polymerization of organic dispersible polyaniline nanoparticles," *Synthetic Metals*, vol. 159, no. 1-2, pp. 123–131, 2009.

[10] N. Chandrakanthi and M. A. Careem, "Thermal stability of polyaniline," *Polymer Bulletin*, vol. 44, no. 1, pp. 101–108, 2000.

[11] H. S. O. Chan, P. K. H. Ho, S. C. Ng, B. T. G. Tan, and K. L. Tan, "A new water-soluble, self-doping conducting polyaniline from poly(o-aminobenzylphosphonic acid) and its sodium salts: synthesis and characterization," *Journal of the American Chemical Society*, vol. 117, no. 33, pp. 8517–8523, 1995.

[12] A. Watanabe, K. Mori, A. Iwabuchi, Y. Iwasaki, Y. Nakamura, and O. Ito, "Electrochemical polymerization of aniline and N-alkylanilines," *Macromolecules*, vol. 22, no. 9, pp. 3521–3525, 1989.

[13] S. S. Pandey, S. Annapoorni, and B. D. Malhotra, "Synthesis and characterization of poly(aniline-co-o-anisidine): a processable conducting copolymer," *Macromolecules*, vol. 26, no. 12, pp. 3190–3193, 1993.

[14] S. Palaniappan and V. Nivasu, "Emulsion polymerization pathway for preparation of organically soluble polyaniline sulfate," *New Journal of Chemistry*, vol. 26, no. 10, pp. 1490–1494, 2002.

[15] S. Bilal, S. Gul, K. Ali, and A. U. A. Shah, "Synthesis and characterization of completely soluble and highly thermally stable PANI-DBSA salts," *Synthetic Metals*, vol. 162, no. 24, pp. 2259–2266, 2012.

[16] T. Chen, C. Dong, X. Li, and J. Gao, "Thermal degradation mechanism of dodecylbenzene sulfonic acid-hydrochloric acid co-doped polyaniline," *Polymer Degradation and Stability*, vol. 94, no. 10, pp. 1788–1794, 2009.

[17] R. K. Paul and C. K. S. Pillai, "Thermal properties of processable polyaniline with novel sulfonic acid dopants," *Polymer International*, vol. 50, no. 4, pp. 381–386, 2001.

[18] C.-H. Chen, "Thermal and morphological studies of chemically prepared emeraldine-base-form polyaniline powder," *Journal of Applied Polymer Science*, vol. 89, no. 8, pp. 2142–2148, 2003.

[19] R. Ansari and M. B. Keivani, "Polyaniline conducting electroactive polymers thermal and environmental stability studies," *E-Journal of Chemistry*, vol. 3, no. 4, pp. 202–217, 2006.

[20] L. Brožová, P. Holler, J. Kovářová, J. Stejskal, and M. Trchová, "The stability of polyaniline in strongly alkaline or acidic aqueous media," *Polymer Degradation and Stability*, vol. 93, no. 3, pp. 592–600, 2008.

[21] S. D. Bompilwar, S. B. Kondwar, V. A. Tabhanea, and S. R. Kargirwar, "Thermal stability of CdS/ZnS nanoparticles embedded conducting polyaniline nanocomposites," *Advances in Applied Science Research*, vol. 1, no. 1, pp. 166–173, 2010.

[22] M. O. Ansari and F. Mohammad, "Thermal stability of HCl-doped-polyaniline and TiO_2 nanoparticles-based nanocomposites," *Journal of Applied Polymer Science*, vol. 124, no. 6, pp. 4433–4442, 2012.

[23] Z. Qiang, G. Liang, A. Gu, and L. Yuan, "Hyperbranched polyaniline: a new conductive polyaniline with simultaneously good solubility and super high thermal stability," *Materials Letters*, vol. 115, pp. 159–161, 2014.

[24] M. Trchová, P. Matějka, J. Brodinová, A. Kalendová, J. Prokeš, and J. Stejskal, "Structural and conductivity changes during the pyrolysis of polyaniline base," *Polymer Degradation and Stability*, vol. 91, no. 1, pp. 114–121, 2006.

[25] S. Bilal, S. Gul, R. Holze, and A. A. Shah, "An impressive emulsion polymerization route for the synthesis of completely and highly conducting polyaniline salts," *Synthetic Metals*. In press.

[26] S. Bilal, A.-U. A. Shah, and R. Holze, "A correlation of electrochemical and spectroelectrochemical properties of poly(*o*-toluidine)," *Electrochimica Acta*, vol. 54, no. 21, pp. 4851–4856, 2009.

[27] O. Ngamna, A. Morrin, A. J. Killard, S. E. Moulton, M. R. Smyth, and G. G. Wallace, "Inkjet printable polyaniline nanoformulations," *Langmuir*, vol. 23, no. 16, pp. 8569–8574, 2007.

[28] S. Kim and I. J. Chung, "Annealing effect on the electrochemical property of polyaniline complexed with various acids," *Synthetic Metals*, vol. 97, no. 2, pp. 127–133, 1998.

[29] S. Radhakrishnan, C. R. K. Rao, and M. Vijayan, "Performance of conducting polyaniline-DBSA and polyaniline-DBSA/Fe_3O_4 composites as electrode materials for aqueous redox supercapacitors," *Journal of Applied Polymer Science*, vol. 122, no. 3, pp. 1510–1518, 2011.

[30] N. V. Blinova, J. Stejskal, M. Trchová, and J. Prokeš, "Polyaniline prepared in solutions of phosphoric acid: powders, thin films, and colloidal dispersions," *Polymer*, vol. 47, no. 1, pp. 42–48, 2006.

[31] S. Palaniappan and C. A. Amarnath, "A novel polyaniline-maleicacid-dodecylhydrogensulfate salt: soluble polyaniline powder," *Reactive and Functional Polymers*, vol. 66, no. 12, pp. 1741–1748, 2006.

[32] A. Dan and P. K. Sengupta, "Preparation and characterization of soluble polyaniline," *Journal of Applied Polymer Science*, vol. 106, no. 4, pp. 2675–2682, 2007.

[33] L. Wei, Q. Chen, and Y. Gu, "Effects of inorganic acid in DBSA-PANI polymerization on transparent PANI-SiO_2 hybrid conducting films," *Journal of Alloys and Compounds*, vol. 501, no. 2, pp. 313–316, 2010.

[34] O. Ramon, E. Kesselman, R. Berkovici, Y. Cohen, and Y. Paz, "Attenuated total reflectance/fourier transform infrared studies on the phase-separation process of aqueous solutions of poly(N-isopropylacrylamide)," *Journal of Polymer Science, Part B: Polymer Physics*, vol. 39, no. 14, pp. 1665–1677, 2001.

[35] M. J. Silva, A. O. Sanches, L. F. Malmonge et al., "Conductive nanocomposites based on cellulose nanofibrils coated with polyaniline-DBSA via in situ polymerization," *Macromolecular Symposia*, vol. 319, no. 1, pp. 196–202, 2012.

[36] J. Yin, X. Xia, and X. Zhao, "Conductivity, polarization and electrorheological activity of polyaniline nanotubes during thermo-oxidative treatment," *Polymer Degradation and Stability*, vol. 97, no. 11, pp. 2356–2363, 2012.

[37] B.-J. Kim, S.-G. Oh, M.-G. Han, and S.-S. Im, "Synthesis and characterization of polyaniline nanoparticles in SDS micellar solutions," *Synthetic Metals*, vol. 122, no. 2, pp. 297–304, 2001.

[38] J. Yang, Y. Ding, G. Chen, and C. Li, "Synthesis of conducting polyaniline using novel anionic Gemini surfactant as micellar stabilizer," *European Polymer Journal*, vol. 43, no. 8, pp. 3337–3343, 2007.